Crystal Structure of Garciniaphenone and Evidences on the Relationship between Keto–Enol Tautomerism and Configuration

by **Felipe T. Martins***[a]), **I. Camps**[a]), **Antônio C. Doriguetto**[a]), **Marcelo H. dos Santos**[a]), **Javier Ellena**[b]), and **Luiz C. A. Barbosa**[c])

[a]) Department of Exact Science, Federal University of Alfenas, UNIFAL-MG, Rua Gabriel Monteiro da Silva 714, Alfenas-MG, 37130-000, Brazil (phone: +55 35 3299-1261; fax: +55 35 3299-1262; e-mail: felipetmartins@yahoo.com.br)

[b]) Institute of Physics of São Carlos, University of São Paulo, CP 369, 13560-970, São Carlos-SP, Brazil

[c]) Chemistry Department, Federal University of Viçosa, 36571-000, Viçosa-MG, Brazil

Garciniaphenone (= *rel*-(1*R*,5*R*,7*R*)-3-benzoyl-4-hydroxy-8,8-dimethyl-1,7-bis(3-methylbut-2-en-1-yl)bicyclo[3.3.1]non-3-ene-2,9-dione; **1**), a novel natural product, was isolated from a hexane extract of *Garcinia brasiliensis* fruits. The crystal structure of **1** as well as the selected geometrical and configurational features were compared with those of known related polyprenylated benzophenones. Garciniaphenone is the first representative of polyprenylated benzophenones without a prenyl substituent at C(5). Notably, the absence of a 5-prenyl substituent has an impact on the molecular geometry. The tautomeric form of **1** in the solid state was readily established by a residual-electronic-density map generated by means of a difference *Fourier* analysis, and there is an entirely delocalized six-membered chelate ring encompassing the keto–enol moiety. The configuration at C(7) was used to rationalize the nature of the keto–enol tautomeric form within **1**. The intermolecular array in the network is maintained by nonclassical intermolecular H-bonds.

Introduction. – *Garcinia brasiliensis* (MART.) PLANCH. and TRIANA, (Syn. *Rheedia brasiliensis*), commonly known as 'bacupari', is used in Brazil as traditional medicine for the treatment of urinary diseases and several types of tumors [1]. *Garcinia* or *Rheedia* is the most abundant genus of the Guttiferae family, and it is known to be rich in oxygenated and prenylated phenol derivatives [2], including xanthones [3], flavonoids [4], phenolic acids [5], and benzophenones [6]. Previous researchers have reported the presence of various biflavonoids including volkensiflavone and fukugetina [7], as well as of prenylated xanthones in MeOH extracts of *G. brasiliensis* roots [2].

Polyprenylated benzophenones are biologically active compounds and common metabolites from the Guttiferae family. Some of them, as for instance guttiferone A (= *rel*-(1*R*,5*R*,7*R*,8*S*)-3-(3,4-dihydroxybenzoyl)-4-hydroxy-8-methyl-1,5,7-tris(3-methylbut-2-en-1-yl)-8-(4-methylpent-3-en-1-yl)bicyclo[3.3.1]non-3-ene-2,9-dione), were isolated from *Symphonia globulifera*, *Garcinia livingstonei*, *Garcinia ovalifolia*, and *Clusia rosea* as HIV-inhibitory compounds [8]. Consequently, numerous studies have screened such substances to uncover a range of pharmacological properties in various biological systems. As a result, it is agreed that polyprenylated benzophenones also possess radical-scavenging properties, inhibit iNOS and COX-2 expression in colon carcinoma, induce apoptosis, and can act as antiulcer, antioxidant, trypanocidal [9–13], anti-inflammatory [14], and antitumoral agents [15]. Another natural polyprenylated

benzophenone, 7-epiclusianone (= *rel*-(1*R*,5*R*,7*R*)-3-benzoyl-4-hydroxy-8,8-dimethyl-1,5,7-tris(3-methylbut-2-en-1-yl)bicyclo[3.3.1]non-3-ene-2,9-dione; **2**), presents vascular effects on the rat aorta [16] and anti-HIV activity [17].

Three prenylated benzophenones obtained from hexane and EtOH extracts from fruits and seeds of *Garcinia brasiliensis* were purified by column chromatography and prep. TLC. The focus of this article is centered on a compound named garciniaphenone (**1**), a previously undescribed natural product that is present only in the fruit (*Scheme*). The two other compounds, 7-epiclusianone (**2**; *Scheme*) [18] and guttiferone A [8], have already been extracted from other plants of the same family and can also be obtained from *G. brasiliensis* seeds. In contrast to guttiferone A, which is found only in the seeds (isolated from the EtOH extract, see [20]), compound **2** constitutes the major secondary metabolite extracted from the fruits of this species. The crystal structures of compound **2** [18] and guttiferone A [19][20] are known.

Scheme. a) *Keto–Enol Tautomers of Garciniaphenone* (**1**) *in* $CDCl_3$ *Solution* [21] *Showing the same Atom Numbering* (arbitrary) *as for the XRD Structure Representation* (*Fig. 1*). b) *The Major Tautomeric Form of 7-Epiclusianone* (**2**) *and Clusianone* (**3**) *in the Solid State*

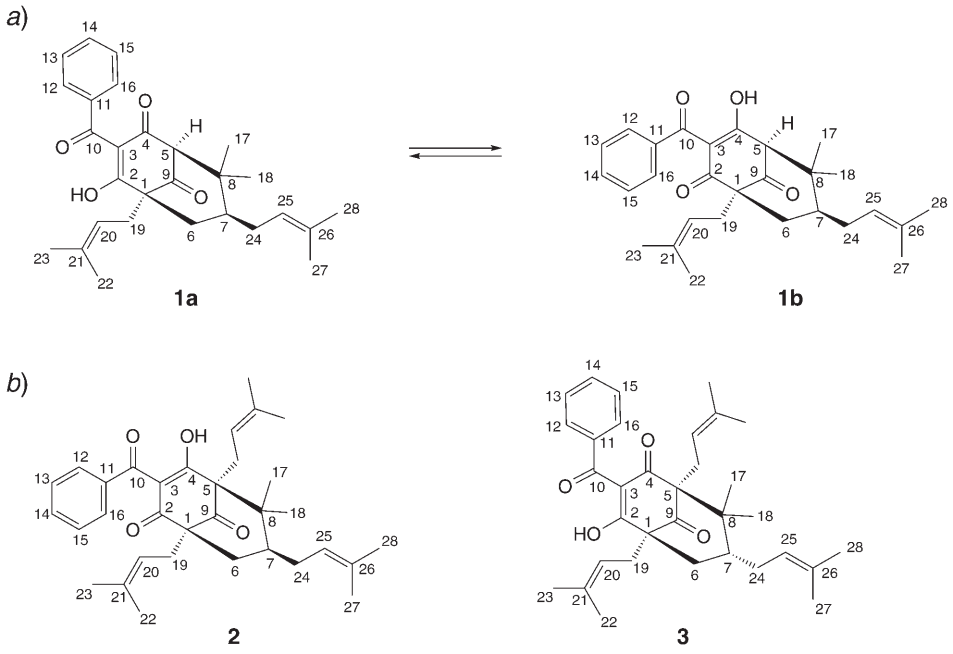

We have studied the chemical structure of compound **1** by IR, ^{1}H-, ^{13}C-, and 2D-NMR, and MS experiments [21]. The NMR spectra of **1** revealed a behavior similar to that of related benzophenones [8], *i.e.*, a keto-enol equilibrium involving the enolizable 2,4-dione system, thus giving rise to ^{1}H-NMR signals of two OH groups from the tautomers **1a** and **1b**, present in solution (*Scheme*). Therefore, the identification of the tautomer present in the solid state was pursued through X-ray diffraction methods,

enabling comparison with solution-state assignments. The X-ray diffraction analysis of **1** was successful, allowing the unambiguous determination of its structure. Furthermore, *ab initio* calculations (6-31G**) were carried out. For this purpose, the XRD structures of **1** and clusianone (**3**; *Scheme*), an analogous polyprenylated benzophenone [22], were used as a starting point for comparative theoretical measurements.

Results and Discussion. – In the HPLC analysis, benzophenones **1** and **2** showed the retention times (t_R) 16.08 ± 0.13 and 17.94 ± 0.06 min, respectively, the peaks exhibiting each a subtle asymmetric shoulder on the tail, which is ascribed to the presence of two keto–enol tautomers [6]. In the chromatograms of samples from the hexane extract of *G. brasiliensis* fruits, a few peaks were present. At the retention times of compounds **1** and **2**, no signal other than chemical background was observed. A linear relationship between the peak-area ratios and dilution concentrations ranging from 0.5 to 40 mg/l was confirmed by the mean correlation coefficients of 0.999 ± 0.001 for **1** and 0.998 ± 0.008 for **2**. The linear equations for **1** and **2** were $y = (0.015 \pm 0.002)x - 0.015 \pm 0.008$ and $y = (0.012 \pm 0.002)x + 0.016 \pm 0.011$, respectively. With these equations and the peak-area ratios obtained from the analyses of the hexane-extract samples, we found 25 ± 2 mg of **1** and 263 ± 40 mg of **2** per g of hexane extract, confirming that the tetraprenylated benzophenone **2** is a major compound in *G. brasiliensis* fruits.

With regard to XRD analysis, the ORTEP-3 [23] representation of garciniaphenone (**1**; *Fig. 1*) shows the absence of a prenyl group at C(5) in comparison with **2**. Unusually, **1** is the first polyprenylated benzophenone in its class lacking a C(5) prenyl substituent. The configuration at C(7) is the same in benzophenones **1** and **2**, the prenyl-group atoms (C(24) to C(28)) laying above the plane passing through atoms C(1), C(5), and C(7) in an axial orientation. This configurational feature causes other similarities between these two structures: the occurrence of the C(10)=O(2)/C(4)–O(1)–H tautomer in the solid state and the spatial orientation of the Bz group on the C(3)–C(10) bond axis. The axial prenyl moiety approaches the C(25)=C(26) and C(2)=O(3) groups, generating an intramolecular distance between the centroid of C(25)=C(26) and O(3) of 3.455(3) Å in **1** and of 3.734(4) Å in **2** [18]. Thus in both cases, the closeness between these groups hinders the binding of C(2)=O(3) to the H-atom deviating the covalent H-bond to O(1), which forms the O(1)–H group. Therefore, the molecular stabilization occurs by an O(1)–H···O(2) H-bond that causes the rotation of the C(3)–C(10) axis. This influence of the C(7) configuration is apparent when considering clusianone (**3**) [22], the epimer of compound **2**, for which the benzoyl group is rotated about 180° around the C(3)–C(10) axis in comparison with structures **1** and **2**. In this case, the equatorial orientation of the C(24)–C(28) prenyl group (below the C(1)–C(5)–C(7) plane) keeps the C(25)=C(26) moiety remote from the C(2)=O(3) group (distance of 5.321 Å between the C(25)=C(26) centroid and O(3)). Thereby, the covalent O–H bond occurs at O(3) that is not sterically hindered, in contrast to structures **1** and **2**. Subsequently, the benzoyl group is rotated to stabilize the structure *via* the O(3)–H···O(2) H-bond.

We also performed *ab initio* calculations in search for theoretical data that could be correlated to structural features established by XRD analysis. Analyzing the quantum-chemical values of the overall energy content E, the HOMO, LUMO, and HOMO–LUMO gap energies, and the dipole moment (μ) of compounds **1** and **3** (*Table 1*),

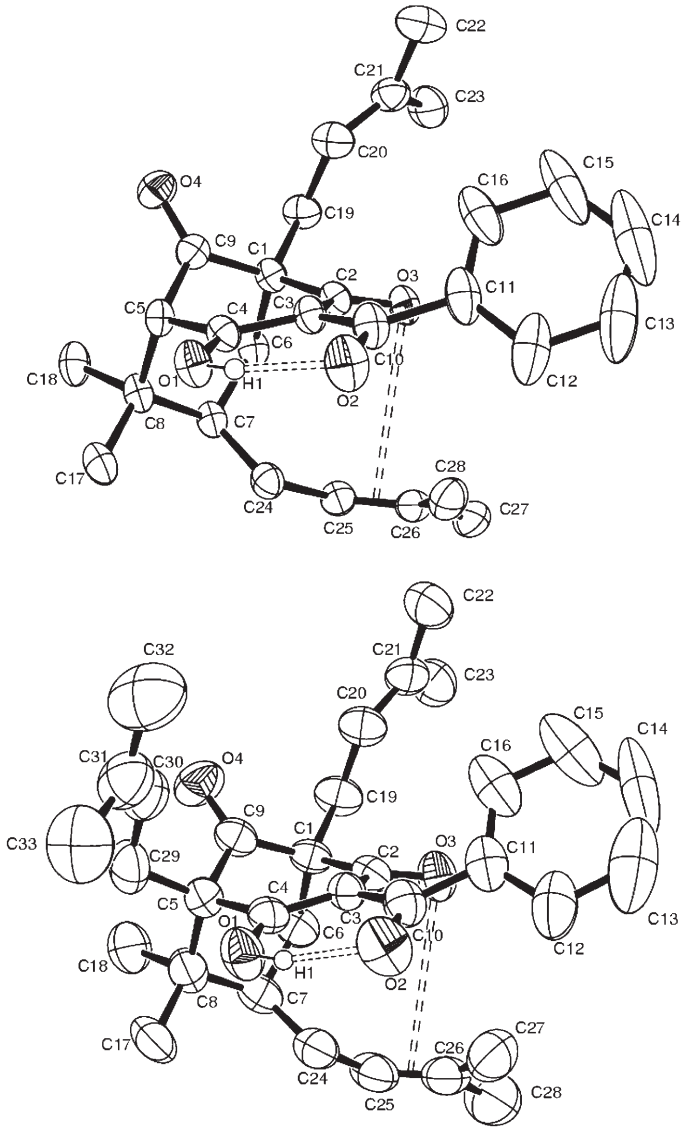

Fig. 1. *ORTEP View of compounds* **1** *and* **2** [18]. Arbitrary atom numbering; 50% probability ellipsoids. Doubly dotted lines represent either the intramolecular H-bond or the contact between the C(25)=C(26) centroid and O(3). The C–H H-atoms are omitted for clarity.

Table 1. *Values of some Quantum-Chemical Properties Calculated for Compounds* **1** *and* **3**

	E [Hartree]	E_{HOMO} [eV]	E_{LUMO} [eV]	$E_{HOMO-LUMO}$ gap [eV]	μ [Debye]
1	– 1379.06	– 8.74	1.95	10.69	2.81
3	– 1573.17	– 8.81	1.93	10.78	1.54

reveals that all values, except for the dipole moment, are similar for the two benzophenones. The difference between the μ values of **1** and **3** is expected, taking into account that **1** is devoid of a prenyl group at C(5).

The benzene ring of **1** has bond angles and distances in agreement with the expected ones (mean C–C distance 1.37(3) Å and mean C–C–C angle 120.0(16)°), the individual values for angles and distances being highly similar. This ring, as expected, is planar, and the largest deviation from the least-squares plane through the six ring C-atoms is 0.031(7) Å for C(14) (r.m.s. deviation of fitted atoms = 0.0185 Å). The C(10)=O(2) group is nonconjugated with the benzene ring due to the reduced planarity between these groups, as shown by the deviation of −0.830(7) Å of O(2) from the ring least-squares plane and by the torsional angle of 43.7(3)° between C(10)=O(2) and the aromatic plane. On the other hand, the C(10)=O(2) group participates in a electronically delocalized six-membered chelate ring formed by O(2)–C(10)–C(3)–C(4)–O(1)–H, which is almost entirely planar, the highest deviation of C(10) from the least-squares plane formed by these six atoms being −0.043(3) Å (r.m.s. deviation of fitted atoms = 0.0466 Å). This result arises from the aromatic character of the chelate ring, which is stabilized by a resonance-assisted H-bond (RAHB) [24]. In this kind of H-bond, the multiple neighboring π-bonds are electronically delocalized, leading to an increase of the H-bonding strength by cooperativity [25]. Moreover, some researchers believe that RAHB-stabilized structures are aromatic [26][27], supporting our above-mentioned idea that was proposed based on geometrical parameters.

The intramolecular geometry in the chelate moiety, as well as the geometry of the entire molecule **1**, was analyzed with MOGUL [28], which confirmed the delocalized resonance character of the chelate ring by the variations in the valence angles and bond distances (*Tables 2* and *3*). The bonds C(3)–C(10) (1.425(4) Å) and C(4)–O(1) (1.285(3) Å) are markedly shorter than the corresponding average query values (1.48(3) and 1.32(3) Å, resp.), whereas the bond C(10)=O(2) (1.270(4) Å) is longer than the value 1.22(2) Å averaged over 2995 structures similar to **1** found by MOGUL in the *Cambridge Structural Database* (*CSD*) [29]. These deviations from the most common bond-distance values are consistent with a complete electronic delocalization within the O(2)–C(10)–C(3)–C(4)–O(1)–H moiety that in solution leads to the two tautomers **1a** and **1b** (*Scheme*). Thus, the C(3)–C(10) and C(4)–O(1) single bonds possess double-bond character, and the C(10)=O(2) double bond has single-bond character. Furthermore, the H-bond to O(2) of C(10)=O(2) in the hybrid resonance structure is also suggested by the enlargement of the C(3)–C(10)–C(11) angle, which supports the C(10)=O(2) group. This angle (124.3(3)°) is greater than the corresponding average angle around a carbonyl group C–C(=O)–C (120(2)°). In turn, the adjoining angle O(2)–C(10)–C(11) is contracted (116.6(3)° *vs.* the mean value of 120(2)° in the *CSD*). The intramolecular H-bond O(1)–H···O(2) also disturbs the valence angles within the hybrid keto–enol ring system. The close proximity of C(10)=O(2) and C(4)–O(1) due to the intramolecular H-bond, as shown by the relatively short intramolecular O(1)···O(2) distance (2.409 (4) Å, *cf. Table 4*), distorts the C(3)–C(10) bond towards the centroid of the chelate ring. As expected for this independent displacement, it does not influence the O(2)–C(10)–C(3) angle (119.0(3)° for **1** *vs.* an average of 119(2)° for 161 **1**-like entries in the *CSD*), whereas

Table 2. *Bond Lengths* [Å] *of Compound* **1** *Determined by XRD* (query value) *and MOGUL Intramolecular Analysis.* For atom numbering, see *Scheme* and *Fig. 1.*

	Number	Mean	Query value		Number	Mean	Query value
C(1)–C(2)	7	1.51(1)	1.527(4)	C(12)–C(13)	10000	1.38(2)	1.395(10)
C(2)–C(3)	103	1.44(2)	1.472(4)	C(13)–C(14)	10000	1.37(3)	1.29(2)
C(3)–C(4)	18	1.39(2)	1.405(4)	C(14)–C(15)	10000	1.37(2)	1.426(16)
C(4)–C(5)	2	1.52(1)	1.497(4)	C(15)–C(16)	10000	1.38(2)	1.374(6)
C(5)–C(8)	7	1.55(1)	1.545(4)	C(11)–C(16)	10000	1.38(1)	1.362(8)
C(7)–C(8)	22	1.54(1)	1.545(4)	C(24)–C(25)	171	1.49(2)	1.497(4)
C(6)–C(7)	271	1.53(1)	1.530(4)	C(25)–C(26)	361	1.31(3)	1.319(5)
C(1)–C(6)	59	1.53(1)	1.516(4)	C(26)–C(27)	1140	1.49(3)	1.500(5)
C(1)–C(9)	15	1.53(1)	1.492(4)	C(26)–C(28)	1140	1.49(3)	1.480(6)
C(1)–C(19)	76	1.55(4)	1.525(4)	C(19)–C(20)	152	1.49(3)	1.485(5)
C(3)–C(10)	161	1.48(3)	1.425(4)	C(20)–C(21)	361	1.31(3)	1.309(5)
C(5)–C(9)	9	1.51(1)	1.495(4)	C(21)–C(22)	1140	1.49(3)	1.458(6)
C(8)–C(17)	3573	1.52(3)	1.516(4)	C(21)–C(23)	1140	1.49(3)	1.494(6)
C(8)–C(18)	3573	1.52(3)	1.537(4)	O(1)–C(4)	105	1.32(3)	1.285(3)
C(7)–C(24)	24	1.54(1)	1.503(4)	O(2)–C(10)	2995	1.22(2)	1.270(4)
C(10)–C(11)	915	1.48(3)	1.471(5)	O(3)–C(2)	1225	1.21(2)	1.203(3)
C(11)–C(12)	10000	1.38(1)	1.358(7)	O(4)–C(9)	1247	1.20(2)	1.203(4)

Table 3. *Bond Angles* [°] *of Compound* **1** *Determined by XRD* (query value) *and MOGUL Intramolecular Analysis.* For atom numbering, see *Scheme* and *Fig. 1.*

	Number	Mean	Query value		Number	Mean	Query value
C(1)–C(2)–C(3)	19	119(2)	118.0(2)	C(9)–C(1)–C(19)	27	108(2)	113.9(3)
C(1)–C(6)–C(7)	7	114(1)	117.5(2)	C(10)–C(11)–C(12)	1762	120(2)	119.4(5)
C(1)–C(9)–C(5)	16	116(2)	113.5(3)	C(10)–C(11)–C(16)	1762	120(2)	120.6(4)
C(1)–C(19)–C(20)	27	113(2)	112.3(3)	C(11)–C(12)–C(13)	10000	120(1)	117.7(8)
C(2)–C(1)–C(6)	15	108(1)	108.4(2)	C(11)–C(16)–C(15)	10000	120(1)	122.4(7)
C(2)–C(1)–C(9)	23	111(3)	110.3(2)	C(12)–C(11)–C(16)	10000	118(1)	119.8(5)
C(2)–C(1)–C(19)	9	109(2)	109.4(2)	C(12)–C(13)–C(14)	10000	120(1)	123.3(11)
C(2)–C(3)–C(4)	15	120(1)	118.4(2)	C(13)–C(14)–C(15)	10000	120(2)	120.1(7)
C(2)–C(3)–C(10)	**15**	**119(3)**	**123.0(2)**	C(14)–C(15)–C(16)	10000	120(1)	116.3(9)
C(3)–C(4)–C(5)	15	119(4)	122.3(2)	C(17)–C(8)–C(18)	510	107(1)	106.9(3)
C(3)–C(10)–C(11)	**147**	**120(2)**	**124.3(3)**	C(24)–C(25)–C(26)	26	128(2)	126.9(3)
C(4)–C(3)–C(10)	**15**	**121(2)**	**117.9(2)**	C(25)–C(26)–C(27)	722	122(3)	120.1(4)
C(4)–C(5)–C(8)	2	113.7(2)	116.7(3)	C(25)–C(26)–C(28)	722	122(3)	124.8(4)
C(4)–C(5)–C(9)	68	107(3)	107.2(2)	C(27)–C(26)–C(28)	570	114(2)	115.0(4)
C(5)–C(8)–C(7)	24	107(2)	110.9(2)	C(19)–C(20)–C(21)	73	128(4)	127.3(4)
C(5)–C(8)–C(17)	14	109(2)	109.3(2)	C(20)–C(21)–C(22)	722	122(3)	121.7(4)
C(5)–C(8)–C(18)	14	109(2)	107.3(3)	C(20)–C(21)–C(23)	722	122(3)	122.7(4)
C(8)–C(5)–C(9)	149	110(2)	108.2(2)	C(22)–C(21)–C(23)	570	114(2)	115.5(4)
C(8)–C(7)–C(6)	4	110(1)	112.0(2)	O(1)–C(4)–C(3)	18	122(1)	122.0(3)
C(8)–C(7)–C(24)	6	115(1)	113.7(2)	O(1)–C(4)–C(5)	18	113(3)	115.7(2)
C(7)–C(8)–C(17)	44	109(2)	114.0(3)	O(2)–C(10)–C(3)	161	119(2)	119.0(3)
C(7)–C(8)–C(18)	44	109(2)	108.1(3)	**O(2)–C(10)–C(11)**	**915**	**120(2)**	**116.6(3)**
C(7)–C(24)–C(25)	18	114(3)	113.1(3)	O(3)–C(2)–C(1)	7	119(2)	119.0(2)
C(6)–C(1)–C(9)	33	107(2)	105.7(2)	O(3)–C(2)–C(3)	103	123(2)	123.0(3)
C(6)–C(1)–C(19)	7	111(1)	109.0(2)	**O(4)–C(9)–C(1)**	**15**	**121(1)**	**124.9(3)**
C(6)–C(7)–C(24)	7	109(1)	114.3(2)	O(4)–C(9)–C(5)	9	123(1)	121.6(3)

Table 4. *H-Bonding Length* [Å] *and Angles* [°] *of Compound* **1**. The symbols 'D' and 'A' mean H-atom donor and acceptor, resp. For atom numbering, see *Scheme* and *Fig. 1*

D–H···A	D–H	H···A	D···A	D–H···A
O(1)–H···O(2)	1.06(5)	1.40(6)	2.409(4)	156(5)
C(6)–H_b···O(2)[a])	0.97	2.60	3.515(4)	158
C(14)–H···O(3)[b])	0.93	2.53	3.414(8)	159
C(25)–H···O(4)[c])	0.93	2.74	3.632(5)	161
C(28)–H_c···O(3)	0.96	2.57	3.351(5)	139

[a]) Symmetry: $x+1, y, z$. [b]) Symmetry: $x-½, -y+½, -z$. [c]) Symmetry: $-x+2, y-½, -z+½$

the angle C(2)–C(3)–C(10) is relaxed (123.0(2)° *vs.* 119(3)°) and the angle C(4)–C(3)–C(10) is constrained (117.9(2)° *vs.* 121(2)°).

In guttiferone A, a benzophenone structurally related to compound **1**, which carries a 3-(3,4-dihydroxybenzoyl) instead of the 3-benzoyl group, and which is present in the *G. brasiliensis* seeds, the OH group in 4-position of the aromatic ring allows a further electron delocalization within the 4-HO–C_6H_3(OH)–C(11)–C(10)–O(2) moiety that enhances the electron density at O(2) [20]. Thus, O(2) rather than O(1) is covalently bonded to the H-atom, and the keto–enol tautomer with the C(10)–O(2)–H/C(4)=O(1) structure was found to contribute most to the solid state of guttiferone A, in contrast to the prevailant tautomer with the C(10)=O(2)/C(4)–O(1)–H moiety determined here in the crystal structure of **1**.

In the bicyclic system of **1**, the six-membered rings C(5)–C(8)–C(7)–C(6)–C(1)–C(9) and C(1)–C(2)–C(3)–C(4)–C(5)–C(9) adopt a chair and distorted half-chair conformation, respectively. The bond length C(5)–C(8) is 1.545(4) Å. This value is shorter than the corresponding C(5)–C(8) distance of **3** (1.603 Å) [22] and **2** [18]. The reduced C(5)–C(8) bond length in **1** is explained by the reduced steric congestion at C(5) due to the absence of the 5-prenyl substituent, as compared to **2** and **3**. Additionally, the absence of the 5-prenyl group is also responsible for the opening of the O(4)–C(9)–C(1) angle (124.9(3)° *vs.* the query mean value 121(1)°). Indeed, the bulky 5-prenyl group sterically repulses the C(9)=O(4) group in the direction of the C(1)–C(9) bond spatial domain, thereby contracting the O(4)–C(9)–C(1) angle and opening the O(4)–C(9)–C(5) angle. A slight closing of the O(4)–C(9)–C(5) angle in **1** was also verified by MOGUL [28] (121.6(3)° *vs.* the query mean value 123(1)°).

The chelate ring in **1** is stabilized through the intramolecular H-bond O(1)–H···O(2) responsible for the Bz group rotation (*Fig. 1*, *Table 4*). It is important to emphasize that the noncovalent O(2)···H(1) bond can be considered as an unusual covalent O–H bond since it belongs to a RAHB in a six-membered chelate ring. As to the intermolecular geometry, compound **1** exhibits four nonclassical intermolecular H-bonds. Two of them, the C(14)–H···O(3) H-bond between the benzene ring and the adjacent C(2)=O(3) and the C(6)–H_b···O(2) H-bond between C(6) of the bicyclic moiety and C(10)=O(2) belonging to Bz moiety, stabilize the molecules along the [100] direction in a stacking mode, forming an infinite ribbon in this direction (*Fig. 2*). The intermolecular C(25)–H···O(4) H-bond between the sp^2-hybridized C(25) of the

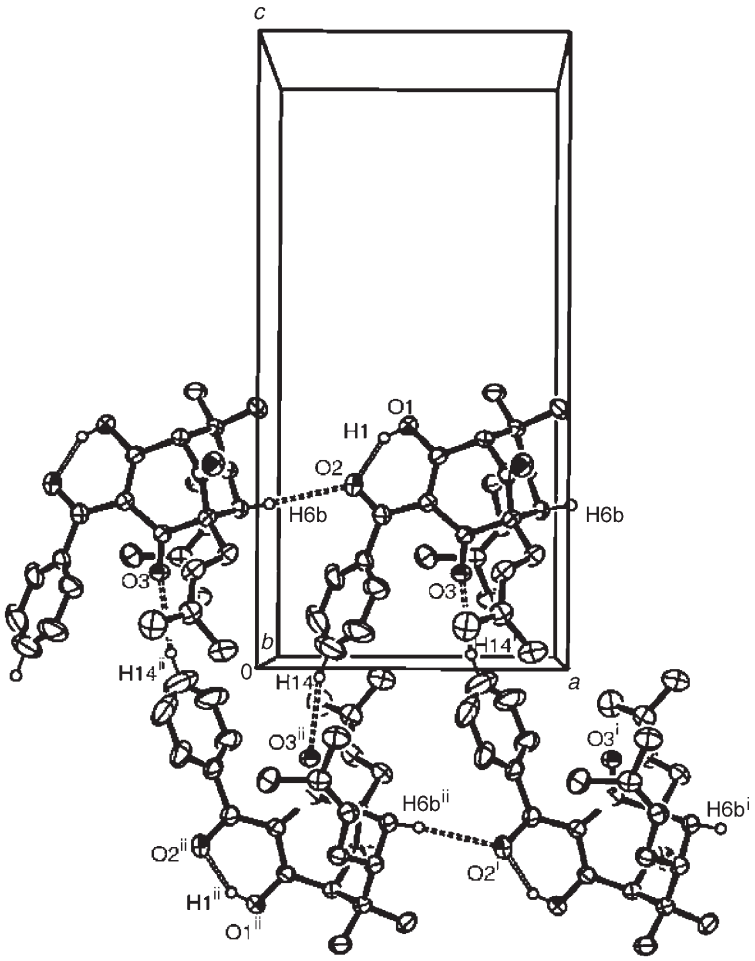

Fig. 2. *Crystal packing view of compound* **1** *along the [100] direction.* Doubly dotted lines represent H-bonds. The H-atoms involved in the H-bonds are shown as spheres of arbitrary radii. Symmetry codes: *i*) $x+½;\ -y+½;\ -z$; *ii*) $x-½;\ -y+½;\ -z$.

prenyl group at C(7) and C(9)=O(4) gives rise to a molecular zigzag chain parallel to the [010] direction (*Fig. 3*). Details of all intermolecular H-bonds interactions involved in these networks are given in *Table 4*.

Conclusions. – The crystal structure of **1**, the first representative without a C(5) prenyl substituent in the class of polyprenylated benzophenones, was determined for the first time, resulting in a correct characterization of the intra- and intermolecular geometries. In the solid state of benzophenone **1**, the C(10)=O(2)/C(4)–O(1)–H tautomer is present, which is the same type of tautomer as in the related natural benzophenone **2** but is different from the C(10)–O(2)–H/C(4)=O(1) tautomer type

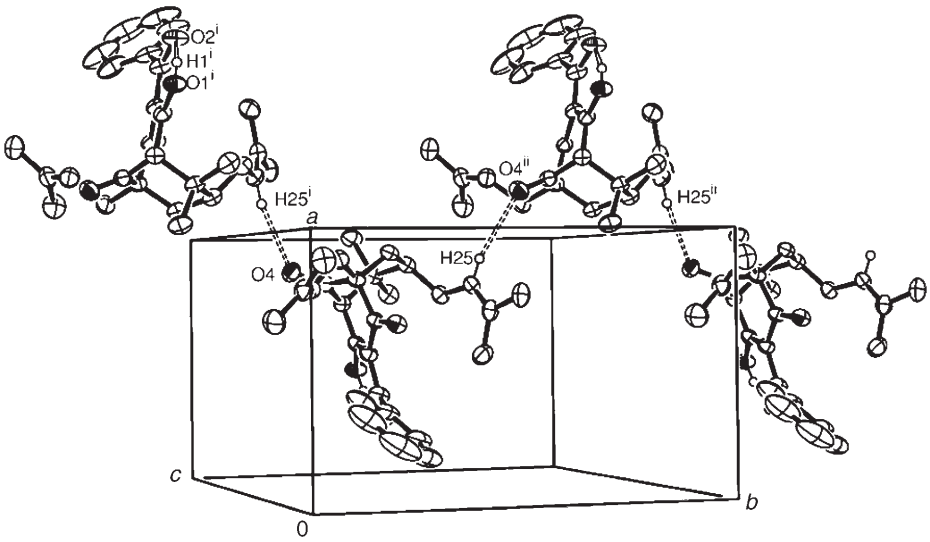

Fig. 3. *Crystal packing view of compound* **1** *along the [010] direction.* Doubly dotted lines represent H-bonds. The H-atoms involved in the H-bonds are shown as spheres of arbitrary radii. Symmetry codes: *i*) $-x+2; y+½; -z+½$; *ii*) $-x+2; y-½; -z+½$.

present in solid guttiferone A. Some changes in bond and torsional angles and bond lengths are reported as a consequence of a delocalized six-membered chelate ring encompassing O(2)–C(10)–C(3)–C(4)–O(1)–H and of the absence of a 5-prenyl substituent in comparison with similar polyprenylated benzophenones. In addition, the reason for the presence of different keto–enol tautomeric forms in the case of **1** and **3** in the solid state is most likely due to the different configuration at C(7).

We thank the *Brazilian Research Council CNPq* (*Conselho Nacional de Desenvolvimento Científico e Tecnológico*) and CAPES (*Coordenação de Aperfeiçoamento de Pessoal de Nível Superior*) for research fellowships (L.C.A.B., A.C.D., J.E., and F.T.M.), FAPEMIG (*Fundação de Amparo à Pesquisa do Estado de Minas Gerais Proc.*, EDT-3310/06), and FINEP (*Financiadora de Estudos e Projetos-Proc.,* 1110/06) for financial support, and the Instituto Rocasolano-CSIC, Spain, for the *CSD* licence.

Experimental Part

Plant Extraction and Isolation of **1**. *Garcinia brasiliensis* fruits were obtained from plants growing naturally on the campus of the Federal University of Viçosa (UFV), Viçosa-MG, Brazil, and their identity was confirmed by a botanist of UFV. The voucher specimen is deposited in the Horto Botânico of UFV (registry No. VIC2604). Subsequently, the air-dried fruits were powdered, yielding *ca.* 1 kg of plant material. After standing maceration with 3 l of hexane at r.t. for 7 d, the liquid layer was recovered by filtration and the hexane evaporated at 45°. The overall procedure was repeated five times on the same batch of material to yield a total amount of 80 g of *G. brasiliensis* fruit hexane extract (GBFHE). The GBFHE was subjected to repeated column chromatography (CC) (silica gel (230–400 mesh), 8 × 100 cm columns, hexane/AcOEt 100:0 → 0:100 and AcOEt/EtOH 100:0 → 0:100). The obtained 50 fractions were grouped to *GBFHE-1* (*Frs. 1–6*, 10 g, mixture of sesquiterpenes by GC/MS), *GBFHE-2* (*Frs. 7–20*, 20 g, resinous orange material), and *GBFHE-3* (*Frs. 21–50*, 30 g, complex mixture by GC/MS). *GBFHE-2* was washed with acetone to produce two subfractions, the insoluble *GBFHE-2I* (5 g of a

hydrocarbon mixture and the soluble *GBFHE-2S*. From *GBFHE-2S*, a yellow resinous material was separated after solvent evaporation. *GBFHE-2S* was subjected to CC (SiO_2) as described previously [21], giving 26 fractions that were pooled into 5 main fractions: *GBFHE-2S.1 – 5*. Three recrystallizations of *GBFHE-2S.3* (1.8 g) in MeOH gave 7-epiclusianone (**2**; 1 g), identified by comparison with reported data [18][30]. *GBFHE-2S.4* (8.0 g) was resubjected to CC (SiO_2) to give 20 fractions, which were pooled into 7 main fractions: *GBFHE-2S.4.A – G*. Recrystallization of *GBFHE-2S.4.A – B* from MeOH (yielded more **2** (1.0 g). *GBFHE-2S.4.C* was recrystallized twice from MeOH: garciniaphenone (**1**; 0.65 g).

Crystal Purity and Quantification of Garciniaphenone (= rel-*(1*R*,5*R*,7*R*)-3-Benzoyl-4-hydroxy-8,8-dimethyl-1,7-bis(3-methylbut-2-en-1-yl)bicyclo[3.3.1]non-3-ene-2,9-dione*; **1**) *and 7-Epiclusianone* (= rel-*(1*R*,5*R*,7*R*)-3-Benzoyl-4-hydroxy-8,8-dimethyl-1,5,7-tris(3-methylbut-2-en-1-yl)bicyclo[3.3.1]non-3-ene-2,9-dione*; **2**). To prepare suitable standards for chromatographic analysis, crystals of benzophenones **1** and **2** were weighed (11 and 12 mg, resp.) and dissolved in MeOH (10 ml) (1.1 and 1.2 g/l). These solns. were diluted in MeOH/5% AcOH soln. (pH 3.84) 40:60 (*v*/*v*; HPLC initial mobile phase) to give standard solns. containing 40.0, 20.0, 10.0, 5.0, and 0.5 mg/l. Three samples of 20 µl (loop capacity) of each standard soln. were analyzed by HPLC (*Shimadzu Corporation* (Kyoto, Japan) apparatus, two *LC-10ATvp* pumps, *SPD-M10Avp* diode array detector at 254 nm, *C18* column (150 mm × 4.6 mm with 5 µm particle size) protected by a compatible guard column; gradient MeOH/5% AcOH soln. (pH 3.84) 40:60 (*v*/*v*) → MeOH within 10 min, flow rate 1.2 ml/min, 30°). Prior to use, the mobile-phase solvents were filtered under vacuum through a 0.45 µm *Millipore* filter (*HAWP 01300*) and degassed separately. ClassVP-LC10 software was used both for data collection and acquisition. All HPLC plots of the standard solns. of **1** and **2** showed only a single strong signal, the means and standard deviations of the percent areas from all dilutions being 98.6 ± 1.1 and $99.8 \pm 0.2\%$, resp. The purity of **1** and **2** was thus considered suitable for an anal. standardization, and the standard solns. were used to generate calibration curves.

The quantification of **1** and **2** in GBFHE extracts was carried out by HPLC in triplicate under the same conditions as those employed in the HPLC analyses of the standard solns. (*cf.* above). The standard curves were derived by linear-regression analysis of the peak-area ratios (analyte/internal standard) *vs.* concentrations of the dilution, and the peak-area ratios of compounds **1** and **2** in the GBFHE samples were interpolated in the generated calibration curves for quantification. Prior to injection, the GBFHE sample (0.727, 0.689, and 0.750 g, resp.) was separately treated with MeOH (*ca.* 5 ml) at 40° during 10 min, the soln. quantitatively filtered through *Whatman®-41* filter paper, and the filtrate made up to 10 ml with MeOH. From this soln., a sample (25 µl) was diluted to a final volume of 10 ml with MeOH/5% AcOH soln. (pH 3.84) 40:60 (*v*/*v*). An internal standard ((2,4-dihydroxyphenyl)(2-hydroxyphenyl)methanone) [31], 10 g/l in MeOH) was added (final concentration, 100 mg/l) to each final 10 ml of calibration standard solns. and GBFHE-sample solns.

X-Ray Diffraction (XRD) *Experiment*[1]). A suitably shaped and sized clear single crystal of **1** was selected for the XRD experiment. The intensity data were measured up to 56.24° in 2θ with the crystal at r.t. (293 K) and with graphite monochromated MoK_α radiation (λ 0.71073 Å), by using the *Enraf-Nonius-Kappa-CCD* diffractometer. The cell refinements were achieved with the Collect [32] and Scalepack [33] softwares. The final cell parameters were obtained from all 20638 reflections. Data integration and scaling were carried out with the Denzo-SMN and Scalepack [33] softwares. No absorption correction was required due to a negligible absorption coefficient of 0.079 mm^{-1} for **1**. The structure was solved with SHELXS-97 [34] and refined with SHELXL-97 software [35]. The C- and O-atoms were clearly solved, and full-matrix least-squares refinement of these atoms with anisotropic thermal parameters was carried out. The CH H-atoms were positioned according to the configuration and were refined with fixed individual displacement parameters ($U_{iso}(H) = 1.2U_{eq}$ (C_{sp^2}) or $1.5U_{eq}$ (C_{sp^3})) by means of a riding model with aromatic C–H bond length of 0.93 Å, methyl C–H bond length of 0.96 Å, methylene C–H bond length of 0.97 Å, and methine C–H bond length of 0.98 Å. The OH H-

---

[1]) CCDC-667556 contains the supplementary crystallographic data for this paper. These data can be obtained free of charge *via* http://www.ccdc.cam.ac.uk/data_request/cif (or from the *Cambridge Crystallographic Data Centre*, 12 Union Road, Cambridge CB21EZ, UK; fax: +44 1223 336033; e-mail: deposit@ccdc.cam.ac.uk).

atom was located by difference *Fourier* analysis and was set as isotropic. For that, the positional parameter of this H-atom was not constrained during refinements. Crystal, collection, and structure refinement data are summarized in *Table 5*.

Table 5. *Crystallographic Data of Compound* **1**

Empirical formula		$C_{28}H_{34}O_4$	Absorption coefficient [mm^{-1}]	0.079
M_r		434.55	$F(000)$	936
Crystal dimensions [mm]		$0.1 \times 0.2 \times 0.4$	θ Range for data collection [°]	3.03–28.12
Temperature [K]		293(2)	Index ranges	$-11 \le h \le 11$; $-18 \le k \le 18$; $-22 \le l \le 23$
Wavelength [Å]		0.71073	Reflections collected	20638
Crystal system		orthorhombic	Independent reflections	3110 [$R(\text{int}) = 0.0407$]
Space group		$P2_12_12_1$	Completeness to $\theta = 28.12°$	94.2%
Unit cell parameters	a [Å]	8.9985(3)	Refinement method	Full-matrix least-squares on F^2
	b [Å]	14.4589(6)	Data, restraints, parameters	3110, 0, 294
	c [Å]	18.4322(6)	Goodness-of-fit on F^2	1.045
	V [Å^3]	2398.2(1)	Final R for $I > 2\sigma(I)$	$R_1 = 0.0556$
Z		4	R indices (all data)	$wR_2 = 0.1803$
D_x (calc.) [Mg m^{-3}]		1.204	$\Delta\rho$ (max; min) [e Å^{-3}]	0.246; −0.187

Tables 2–4 were generated by WinGX [36]. ORTEP-3 [23] and MERCURY [37] softwares were used to prepare the crystal-data presentations. The molecular conformation and geometry were studied by MOGUL [28], a knowledge base that processes a molecule submitted either manually or by another computer program *via* an instruction-file interface and performs substructure searches typically involving bond lengths and angles (including torsions) within the *Cambridge Structural Database* (*CSD*) [29].

In spite of **1** crystallizing in a noncentrosymmetric space group, the *Flack* parameter was not refined during X-ray crystallographic analysis. Since the most electron-rich atom is O, which does not have an anomalous scattering large enough (using MoK_α radiation) to permit determination of the absolute structure by X-ray diffraction, *Friedel* pairs were averaged before refinement. In addition, unusual U_{eq} values were observed for C(14) and C(21) due to the presence of a slight static disorder involving the aromatic atoms in the structure. In spite of this, we used the classical harmonic model based upon a development of the atomic displacement parameters (ADP) with just one site instead of the split-position model. It is important to comment that trial refinements were used with the split-atom approach. However, since the extra disordered sites are very close together, high correlation and instable refinements were observed applying the classical split-atom approach to the structural model. From a statistical point of view, the one-site model is better than the split-atom one. The former model also converges easier, which is probably due to lower correlations between the refined ADP and occupancy parameters. Furthermore, high U_{eq} values of aromatic C-atoms are commonly reported for the related benzophenones **2** [18] and **3** [22]. The same argument can be used to explain a larger than usual range of U_{eq} values for H-atoms of **1** since they were refined with fixed individual displacement parameters ($U_{iso}(H) = 1.2U_{eq}(C_{sp^2})$).

Identification of **2**. Compound **2** was identified by both its chromatographic and spectral data, which were identical to those of 7-epiclusianone previously identified by both X-ray diffraction analysis and spectroscopic measurements (UV, IR, NMR, and MS) [18][30].

Molecular Calculations Starting from the XRD Structures of Compounds **1** *and* **3**. The calculations were performed with a two dual core 2-GHz Opteron processor PC computer running Fedora 7 Linux. The quantum calculations were carried out in the gas phase by a full *ab initio Hartree–Fock* methodology with the 6-31G** basis implemented in the GAMESS-US code [38][39]. As input, the geometries determined by the XRD analysis were used without further optimization. The HOMO, LUMO, and the dipole moments for each structure were calculated as implemented in the GAMESS-US program.

REFERENCES

[1] M. P. Corrêa, 'Dicionário das plantas úteis do Brasil e das plantas exóticas cultivadas', Imprensa Nacional, Rio de Janeiro, 1978.
[2] G. D. Monache, B. Botta, J. F. Mello, J. S. B. Coelho, F. Menichini, *J. Nat. Prod.* **1984**, *47*, 620.
[3] G. J. Bennett, H. H. Lee, *Phytochemistry* **1989**, *28*, 967.
[4] E. G. Crichton, P. G. Waterman, *Phytochemistry* **1979**, *18*, 1553.
[5] A. A. L. Gunatilaka, S. Sotheeswaran, H. T. B. Sriyan, E. S. Waight, *Tetrahedron Lett.* **1982**, *23*, 2987.
[6] O. C. Rubio, A. Padron, H. V. Castro, C. Pizza, L. Rastrelli, *J. Nat. Prod.* **2001**, *64*, 973.
[7] B. Botta, M. M. McQuhae, G. D. Monache, F. D. Monache, J. F. Mello, *J. Nat. Prod.* **1984**, *47*, 1053.
[8] K. R. Gustafson, J. W. Blunt, H. G. M. Munro, R. W. Fuller, C. T. McKee, J. H. Cardellina, J. B. McMahon, G. M. Cragg, M. R. Boyd, *Tetrahedron* **1992**, *48*, 10093.
[9] F. Abe, S. Nagafuji, H. Okabe, H. Akahane, E. E. Muñiz, M. H. Reyes, R. R. Chilpa, *Biol. Pharm. Bull.* **2004**, *27*, 141.
[10] M. H. Pan, W. L. Chang, S. Y. Lin-Shiau, C. T. Ho, J. K. Lin, *J. Agric. Food Chem.* **2001**, *49*, 1464.
[11] T. Tanaka, H. Kohno, R. Shimada, S. Kagami, F. Yamaguchi, S. Kataoka, T. Ariga, A. Murakami, K. Koshimizu, H. Ohigashi, *Carcinogenesis* **2000**, *21*, 1183.
[12] F. Yamaguchi, T. Ariga, Y. Yoshimura, H. Nakazawa, *J. Agric. Food Chem.* **2000**, *48*, 180.
[13] F. Yamaguchi, M. Saito, T. Ariga, Y. Yoshimura, H. Nakazawa, *J. Agric. Food Chem.* **2000**, *48*, 2320.
[14] C. Gopalakrishnan, D. Shankaranarayan, S. K. Nazimudeen, L. Kameswaran, *Ind. J. Med. Res.* **1980**, *71*, 940.
[15] D. D. Carballo, S. Seeber, D. Strumberg, R. A. Hilger, *Int. J. Clin. Pharm. Therap.* **2003**, *41*, 622.
[16] A. J. Cruz, V. S. Lemos, M. H. Santos, T. J. Nagem, S. F. Cortes, *Phytomedicine* **2006**, *13*, 442.
[17] A. L. Piccinelli, O. C. Rubio, M. B. Chica, N. Mahmood, B. Pagano, M. Pavone, V. Barone, L. Rastrelli, *Tetrahedron* **2005**, *61*, 8206.
[18] M. H. Santos, N. L. Speziali, T. J. Nagem, T. T. Oliveira, *Acta Crystallogr., Sect. C* **1998**, *54*, 1990.
[19] B. N. Lenta, D. T. Noungoue, K. P. Devkota, P. A. Fokou, S. Ngouela, E. Tsamo, N. Sewalda, *Acta Crystallogr., Sect. E* **2007**, *63*, 1282.
[20] F. T. Martins, J. W. Cruz Jr., P. B. M. C. Derogis, M. H. Santos, M. P. Veloso, J. A. Ellena, A. C. Doriguetto, *J. Braz. Chem. Soc.* **2007**, *18*, 1515.
[21] P. B. M. C. Derogis, F. T. Martins, T. C. Souza, M. E. C. Moreira, J. D. Souza-Filho, A. C. Doriguetto, K. R. Souza, M. P. Veloso, M. H. Santos, *Magn. Reson. Chem.* **2008**, in press.
[22] L. E. McCandlish, J. C. Hanson, G. H. Stout, *Acta Crystallogr., Sect. B* **1976**, *32*, 1793.
[23] L. J. Farrugia, *J. Appl. Crystallogr.* **1997**, *30*, 565.
[24] P. Sanz, O. Mó, M. Yáñez, J. Elguero, *J. Phys. Chem. A* **2007**, *111*, 3585.
[25] L. Sobczyk, S. J. Grabowski, T. M. Krygowski, *Chem. Rev.* **2005**, *105*, 3513.
[26] G. Gilli, F. Bellucci, V. Ferretti, V. Bertolasi, *J. Am. Chem. Soc.* **1989**, *111*, 1023.
[27] G. Gilli, P. Gilli, *J. Mol. Struct.* **2000**, *552*, 1.
[28] I. J. Bruno, J. C. Cole, M. Kessler, J. Luo, W. D. S. Motherwell, L. H. Purkis, B. R. Smith, R. Taylor, R. I. Cooper, S. E. Harris, A. G. Orpen, *J. Chem. Inf. Comput. Sci.* **2004**, *44*, 2133.
[29] F. H. Allen, *Acta Crystallogr., Sect. B* **2002**, *58*, 380.
[30] M. H. Santos, T. J. Nagem, R. Braz-Filho, I. S. Lula, N. L. Speziali, *Magn. Reson. Chem.* **2001**, *39*, 155.
[31] A. C. Doriguetto, F. T. Martins, J. A. Ellena, R. Salloum, M. H. Santos, M. E. C. Moreira, J. M. Schneedorf, T. J. Nagem, *Chem. Biodivers.* **2007**, *4*, 488.
[32] Enraf-Nonius Collect, Nonius BV, Delft, the Netherlands, 1997–2000.
[33] Z. Otwinowski, W. Minor, in 'Methods in Enzymology', Eds. C. W. Carter Jr., and R. M. Sweet, Academic Press, New York, 1997, Vol. 276, p. 307.
[34] G. M. Sheldrick, SHELXS97, Program for Crystal Structure Resolution, University of Göttingen, Germany, 1997.
[35] G. M. Sheldrick, SHELXL97, Program for Crystal Structures Analysis; University of Göttingen, Germany, 1997.
[36] L. J. Farrugia, *J. Appl. Crystallogr.* **1999**, *32*, 837.

[37] I. J. Bruno, J. C. Cole, P. R. Edgington, M. K. Kessler, C. F. Macrae, P. McCabe, J. Pearson, R. Taylor, *Acta Crystallogr., Sect. B* **2002**, *58*, 389.

[38] M. W. Schmidt, K. K. Baldridge, J. A. Boatz, S. T. Elbert, M. S. Gordon, J. H. Jensen, S. Koseki, N. Matsunaga, K. A. Nguyen, S. J. Su, T. L. Windus, M. Dupuis, J. A. Montgomery, *J. Comput. Chem.* **1993**, *14*, 1347.

[39] M. S. Gordon, M. W. Schmidt, in 'Theory and Applications of Computational Chemistry, The First Forty Years', Eds. C. E. Dykstra, G. Frenking, K. S. Kim, and G. E. Scuseria, Elsevier, Amsterdam, 2005, p. 1167.

Received January 25, 2008